August, 1985] © *1985 The Chemical Society of Japan* *Bull. Chem. Soc. Jpn., 58, 2163—2171 (1985)* 2163

Preparation of Vanadium–Phosphorus Mixed Oxide (P/V=1) Catalysts and Their Application to Oxidation of Butane to Maleic Anhydride

Tomoaki SHIMODA,[†] Toshio OKUHARA, and Makoto MISONO*
Department of Synthetic Chemistry, Faculty of Engineering, The University of Tokyo, Hongo, Bunkyo-ku, Tokyo 113

(Received March 28, 1985)

Several vanadium–phosphorus mixed oxides with a P/V ratio=1 have been prepared and the relationships between the structure of catalyst and the catalytic function for the selective oxidation of butane to maleic anhydride were examined. As revealed from XRD, IR, XPS, and redox titration studies, five among them were presumably composed of crystalline single phases, that is, α-$VOPO_4$, β-$VOPO_4$, and $(VO)_2P_2O_7$ as well as unknown phases X_1 and X_2. The valences of the vanadium of these catalysts were close to five, except for $(VO)_2P_2O_7$ (the valence was four). These phases were prepared, respectively, by controlling the kind of precursors and the calcination conditions. The selectivity to maleic anhydride differed markedly among these catalysts, although the rate did not change much when it was normalized to surface area. The selectivity at 440 °C was less than 20% for α- and β-$VOPO_4$, 40% for X_1 and X_2, and 70% for $(VO)_2P_2O_7$. Amorphous phases having V^{4+} were much less selective than $(VO)_2P_2O_7$. No structural changes of the catalysts after use were observed in the cases of α-, β-$VOPO_4$, and $(VO)_2P_2O_7$. Therefore, the effective phase for selective oxidation of butane to maleic anhydride was speculated to be a phase like $(VO)_2P_2O_7$ in which the valence of vanadium is four and the structure is stable under the reaction conditions.

Vanadium–phosphorus mixed oxides are known as catalysts for the selective oxidation of butene to maleic anhydride.[1] Several basic studies have been reported on the active structure of the catalysts,[2] the role of phosphorus,[2–4] and the reaction mechanism.[3] The preferred atomic ratio of phosphorus to vanadium is usually in the range of 1.2 to 2.0.

Recently, certain V–P oxides with a P/V ratio of between 1.0 and 1.2 were found to be efficient catalysts for the selective oxidation of butane, a saturated hydrocarbon, to maleic anhydride.[1,5] Several studies on V–P oxide catalysts in this composition range have also been reported.[6–10] However, in most studies, the V–P oxide catalysts used had various P/V ratios, and they usually contained unknown phases or were mixtures. Therefore, the real active phase for the butane oxidation still remains unclarified, although there are many proposals in patents for the preparation of effective catalysts.[11–14]

It was recently indicated that nearly crystalline phases with P/V ratios close to unity were active and selective for the oxidation of butane.[6,7,10,14] As for V–P oxide with P/V=1, crystalline phases such as α-$VOPO_4$, β-$VOPO_4$, and $(VO)_2P_2O_7$ are known.[15–18] These facts motivated us to study these catalysts in greater detail as an extention of our studies on oxidation catalysts having well-defined bulk structures.

In the present study we attempted (i) to examine more extensively the preparation process of catalysts having single crystalline phases with P/V=1, by using well-defined precursors and (ii) to specify the phase or structure of a catalyst which is efficient for the oxidation of butane. An elucidation of the mechanism of catalytic action and the reason why that phase is effective will be the subjects of following study.

Experimental

1\. *Catalyst Preparation.* 1.1. *Precursors*: Three kinds of V–P–O compounds (P/V=1) with well-defined structures (denoted as P-I, -II, and -III) have been prepared as precursors for catalysts.

(a) $(NH_4)_2[(VO)_2C_2O_4(HPO_4)_2]\cdot 5H_2O$ (P-I). P-I was prepared according to the literature.[19] V_2O_5 powder (0.1 mol) was added gradually with stirring into 400 ml of an aqueous solution of oxalic acid (0.75 mol l^{-1}) at 80 °C. When the solution turned to blue after a few minutes, $NH_4H_2PO_4$ (0.2 mol) was added. A green precipitate was formed while the stirring continued. The precipitate was filtrated, washed with water and acetone, and dried overnight at 100 °C. The obtained solid was confirmed to be $(NH_4)_2[(VO)_2C_2O_4(HPO_4)_2]\cdot 5H_2O$ by comparing X-ray diffraction powder patterns (XRD) with a reference.[19]

(b) NH_4HVPO_6 (P-II). This precursor (P-II) was prepared according to the literature.[15] V_2O_5 powder (0.04 mol) was added to a boiling aqueous solution of $NH_4H_2PO_4$ (0.8 mol in 600 ml H_2O), and boiling was maintained for 30 min. A yellow precipitate was formed after the solution was allowed to stand overnight. The precipitate was filtrated, washed with water and acetone, and dried overnight at 100 °C. The XRD pattern (d/Å: 8.75 (100), 4.60 (2), 4.46 (3.5), 4.41 (3), 4.09 (3), 3.17 (3), 2.95 (15), relative peak intensity in parentheses) indicated that P-II was well crystallized. However, an identification was not made because of the absence of reference data.

(c) $(VO)_2H_4P_2O_9$[20] (P-III-1, 2, and 3). P-III-1 was prepared according to the literature.[14a] V_2O_5 powder (0.1 mol) was added to an aqueous solution (200 ml) of $NH_2OH\cdot HCl$ (0.2 mol, Nakarai Chemicals) and H_3PO_4 (0.2 mol, Koso Chemicals) at 80 °C and was stirred for 1 h, in order to completely reduce V_2O_5. After the solution became a light-blue slurry of about 100 ml, it was evaporated to dryness at 130 °C overnight. A small quantity of water (100 ml) was added to the dried solid and the mixture was boiled for 10 min. A light green precipitate obtained by filtration was washed with water. The structure was confirmed by its XRD pattern with reference to the literature.[20]

P-III-2 was prepared in a similar manner as P-III-I. The

[†] Present address: Mitsui Petrochemical Industries, Ltd.

Table 1. Starting materials of precursors

Precursor		Starting Materials
P-I	$(NH_4)_2[(VO)_2C_2O_4(HPO_4)_2]$	V_2O_5, $(COOH)_2$, $NH_4H_2PO_4$
P-II	NH_4HVPO_6	V_2O_5, $NH_4H_2PO_4$
P-III-1	$(VO)_2H_4P_2O_9$	V_2O_5, $NH_2OH\cdot HCl$, H_3PO_4
P-III-2	$(VO)_2H_4P_2O_9$	V_2O_5, $NH_2OH\cdot HCl$, H_3PO_4, $C_3H_4O_3$
P-III-3	$(VO)_2H_4P_2O_9$	V_2O_4, H_3PO_4

only difference was that ethylene carbonate ($C_3H_4O_3$, Nakarai Chemicals) was added to the solution before concentration in order to eliminate Cl.[14b)] The XRD pattern was very similar to that of P-III-I; however, the peaks were weaker.

P-III-3 was prepared using V_2O_4. A V_2O_4 powder (0.05 mol, Aldrich) was dissolved into an aqueous solution of H_3PO_4 (0.1 mol in 100 ml H_2O) at 80 °C. The resultant blue solution was concentrated at 80 °C with stirring into a green paste. After the green paste was dried at 100 °C, it was placed into water. A light-blue precipitate was obtained upon filtration and washing with water.

Table 1 summarizes the composition and starting materials of the precursors.

1.2 Calcination of Precursors. The precursors were calcined (a) in streams of O_2 or N_2 in a reactor or (b) in air by use of a muffle furnace.

(a) Each precursor (2—5 g) was calcined in Pyrex-tube reactors (10 or 20 mm in diameter) under the flow of oxygen or nitrogen at a prescribed temperature. The heating rate was controlled by adjusting the power, and the temperature was continuously monitored. The flow rate was 100—200 ml min^{-1}. To avoid any blockage of gas flow due to melting, the heating rate was kept low and a wide reactor diameter was adopted.

(b) In the case of any calcination in air, a muffle furnace was used. The heating rate was about 30 °C min^{-1}.

2. Characterization of Catalysts. *2.1 XRD and IR*: XRD powder patterns of precursors and catalysts were recorded using a Rigaku X-ray diffractometer with Cu $K\alpha$ radiation filtered by Ni. The XRD was also measured for the catalysts after use. Infrared spectra were recorded with a spectrometer (JIR-10, FT-IR) using an KBr supporting disc.

2.2 XPS: XPS measurements of fresh and used catalysts were carried out using an ESCA Lab 5 (Vacuum Generator). The excitation was performed with the Mg $K\alpha$ line. Binding energies were referred to the C_{1s} line (285 eV). Samples were evacuated under 10^{-8} Torr (1 Torr=133.3 Pa) at 25 °C in the ESCA chamber.

2.3 Valence of Vanadium: The average oxidation state of vanadium in the catalysts was determined by redox titration.[9)] About 0.1 g of each catalyst was dissolved in 100 ml of 2 M[†] H_2SO_4 at 80 °C. The vanadium (IV or III) content was determined by titration with a solution of $KMnO_4$ (0.1 M). The vanadium (V) content was determined by titration with a solution of a Mohr salt ($FeSO_4\cdot(NH_4)_2SO_4\cdot 6H_2O$, 0.1 M) using diphenylamine as an indicator.

2.4 Surface Area: The surface areas of the catalyst were measured by the BET method (N_2 adsorption).

3. Measurement of Catalytic Activity and Selectivity. The oxidation of butane was carried out using a conventional fixed-bed flow reactor at atmospheric pressure. The reactor was a Pyrex tube (10 mm in diameter) and was externally heated by an electric furnace. The feed gas consisted of 1.5 vol% butane, 17 vol% oxygen and nitrogen (balance). The reaction temperature was from 250 °C to 440 °C. Products containing carbon were maleic anhydride (MA), CO and CO_2. No other products (C_2–C_3 aldehydes and carboxylic acids) were detected (less than 1%). The carbon balance at the stationary state was always almost 95—100%. Maleic anhydride was collected by a cold trap and was determined by titration with 0.1 M NaOH.[6)] Gaseous products were analyzed by a gas chromatograph. It was confirmed, in some cases, that no products other than MA were trapped.

Results

1. Effects of Calcination Conditions on the Structure of V–P Oxide Catalysts. *1.1 Calcination in O_2 or Air*: The structures of the catalysts obtained by calcination in an O_2 or air flow are summarized in Table 2. The results show that the kinds of precursors, the calcination temperature and the heating rate, all, greatly affect the structure of formed catalysts. For example, a high heating rate caused the formation of β-$VOPO_4$ from P-I, while α-$VOPO_4$ was formed from the same precursor using a low heating rate. At an intermediate heating rate, a mixture of α- and β-phase was obtained.

When P-II was calcined at 550 and 600 °C at a low heating rate, a new XRD pattern (d/Å: 4.72 (40), 4.11 (100), 3.15 (30), relative intensity in parentheses) different from either α-, β-$VOPO_4$ or $(VO)_2P_2O_7$ was observed. A high S/N ratio of the XRD peaks, together with the fact that the same XRD patterns were obtained for two samples containing this phase; indicates that this was a single phase. This will be denoted as X_1 in this paper.

The influence of the calcination temperature is seen from the results obtained at a heating rate of 30 °C min^{-1}. The calcination of P-I at 450 °C formed almost an amorphous phase (weak peaks at d/Å : 4.33, 4.17, 3.91, 3.65, 3.50, and 3.10), while after a calcination at 550 or 600 °C, the resultant catalysts were crystalline. This showed that XRD patterns are ascribable to pure β-$VOPO_4$. Changes in the phase with the calcination temperature was also found in the case of P-II. A new phase denoted by X_2 (d/Å : 4.00 (90), 3.66 (45), 3.12 (100), relative intensity in parentheses), was obtained by a low-temperature calcination. X_1 and X_2 were water-soluble and the solution was acidic (pH was 2.37 at about 2 g l^{-1} for X_1 and X_2), while α-, β-$VOPO_4$, and $(VO)_2P_2O_7$ were water-insoluble.

The calcination of P-III-1, 2, containing vanadi-

[†] 1 M=1 mol dm^{-3}.

Table 2. Structures of catalysts obtained by calcination in O_2 or air

Precursor	in	Rate/°C min^{-1}	T/°C	Time/h	Phase formed[a]	Cat. No.[b]
P-I	O_2	2.9	600	10	α-$VOPO_4$	1
	O_2	5.0	600	10	$\alpha+\beta$	
	O_2	6.4	550	10	β-$VOPO_4$	2
	O_2	7.0	600	10	β-$VOPO_4$	3
	Air	30	450	20	Unknown	
	Air	30	550	16	β-$VOPO_4$	
P-II	Air	30	450	20	X_2	6
	Air	30	500	20	$X_1+\beta$	
	O_2	3.3	550	10	X_1	
	O_2	3.3	600	10	X_1	5
	O_2	7.5	550	10	$\beta+X_1$	
	Air	30	600	16	β-$VOPO_4$	4
P-III-1	Air	30	450	20	$(VO)_2P_2O_7+X_1$	
	Air	30	600	20	$\beta+(VO)_2P_2O_7+X_1$	
	O_2	3.0	600	10	Unknown$+X_1+X_2+\alpha$	
P-III-2	Air	30	450	20	$X_1+(VO)_2P_2O_7$	
	Air	30	600	20	$X_1+\beta$	

a) In the case of mixtures, the main phases are given in the first place. b) The catalyst numbers are the same as those in Tables 4 and 5.

Table 3. Structures of catalysts obtained by calcination in N_2[a]

Precursor	Time/h	Phase formed	Cat. No.[b]
P-I	10	Amorphous	7
P-II	6	Amorphous	8
P-III-1	2	$(VO)_2P_2O_7$	9
P-III-2	2	Unknown	
P-III-3	2	$(VO)_2P_2O_7$	

a) 550 °C. heating rate; 10 °C min^{-1}. b) The catalyst numbers are the same as those in Tables 4 and 5.

um(IV) in air or O_2 yielded mixed phases. The content of $(VO)_2P_2O_7$ tended to increase as the calcination temperature decreased or the heating rate increased.

1.2 Calcination in N_2: Table 3 shows the results for the calcination at 550 °C in N_2 with a heating rate of 10 °C min^{-1}. P-I and P-II were converted to amorphous phases, while P-III-1 and P-III-3 readily changed to $(VO)_2P_2O_7$. Less crystalline P-III-2 gave a phase with weak XRD peaks which are not ascribable to $(VO)_2P_2O_7$.

$(VO)_2P_2O_7$ (obtained by the calcination of P-III-1 in N_2) was insoluble in water. However, when it was heated in O_2 (500 °C, 2 h), a part of the solid became soluble in the water and the solution became brown. Figure 1 shows the changes of XRD patterns of P-III-1 and P-III-2 due to these processes. After heating P-III-1 in N_2, a typical XRD pattern due to $(VO)_2P_2O_7$ was found (Fig. 1A). The subsequent treatment with O_2 at 500 °C caused a partial formation of X_1. By washing with water, the intensity of the XRD peaks due to $(VO)_2P_2O_7$ increased by a factor of about 2; no peaks other than $(VO)_2P_2O_7$ appeared. The changes in the XRD peaks during this procedure were clearer in the case of P-III-2, as shown in Fig. 1B. The weight loss observed by washing with water was about 50% for the latter case.

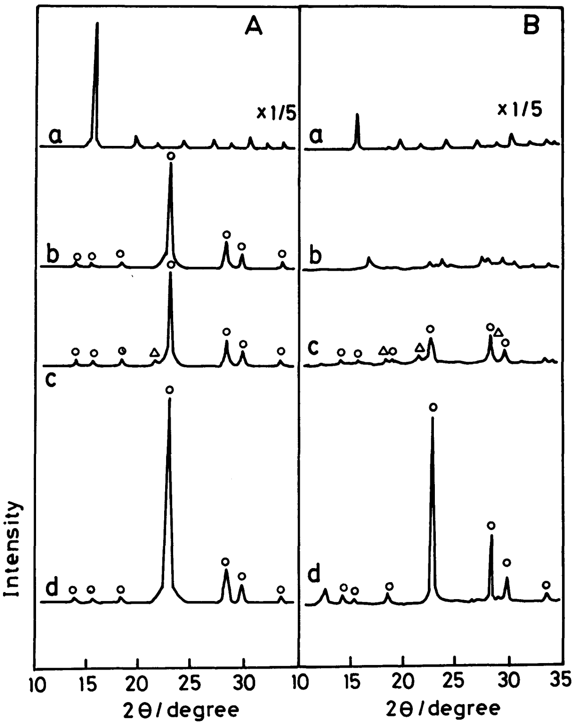

Fig. 1. Changes of XRD patterns by calcination and washing water.
A: P-III-1, B: P-III-2. ○; $(VO)_2P_2O_7$, △; X_1.
a) Precursors, b) After calcination at 550 °C in N_2, c) After calcination at 550 °C in O_2, d) After washing with H_2O.

2. Characterization of Catalyst. The surface area of catalysts and the valence state of vanadium are summarized in Table 4. The surface area decreased as follows: X_1, $X_2>(VO)_2P_2O_7>\alpha$-$VOPO_4>$Amorphous$\geq\beta$-$VOPO_4$. The oxidation states were close to five for α-, β-$VOPO_4$, X_1, and X_2 and that of $(VO)_2P_2O_7$ was essentially four. The valence was lower than four after P-I and P-II were heated in N_2 at 550 °C.

Typical XRD patterns of these phases are shown

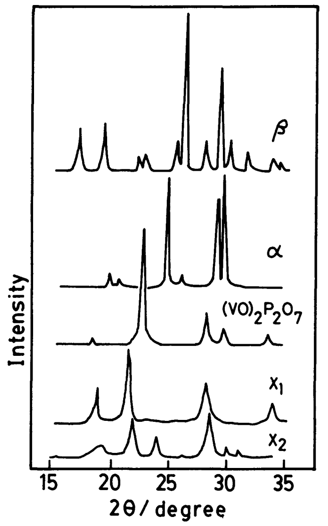

Fig. 2. Typical XRD patterns of V–P oxides prepared.

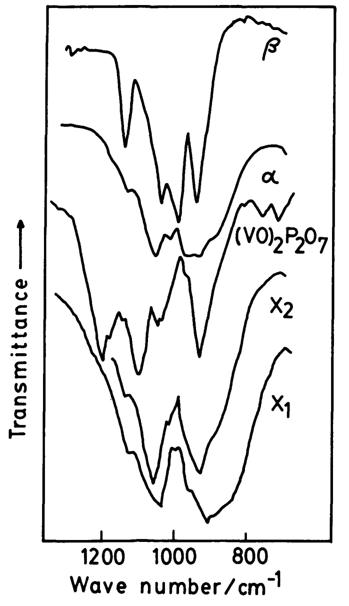

Fig. 3. Infrared spectra of V–P oxides prepared.

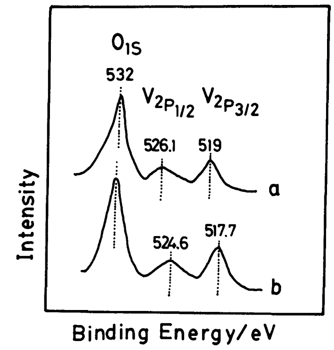

Fig. 4. XPS spectra of β-$VOPO_4$ and $(VO)_2P_2O_7$. a): β-$VOPO_4$, b): $(VO)_2P_2O_7$.

TABLE 4. SURFACE AREAS AND VALENCE STATES OF VANADIUM OF CATALYSTS

Phase	Surface area/m^{2}g^{-1}	Valence of Vanadium	Cat. No.
α-$VOPO_4$	5.9	4.97	1
β-$VOPO_4$	3.4	—	2
β-$VOPO_4$	1.7	4.99	3
β-$VOPO_4$	1.3	—	4
X_1	16.0	4.96	5
X_2	14.1	4.96	6
Amorphous	3.8	3.34	7
Amorphous	3.5	3.77	8
$(VO)_2P_2O_7$	7.1	4.02	9
$(VO)_2P_2O_7$$^{a)}$	12.4	4.00	10

a) After O_2-treatment at 500°C, washing with H_2O, and recalcination.

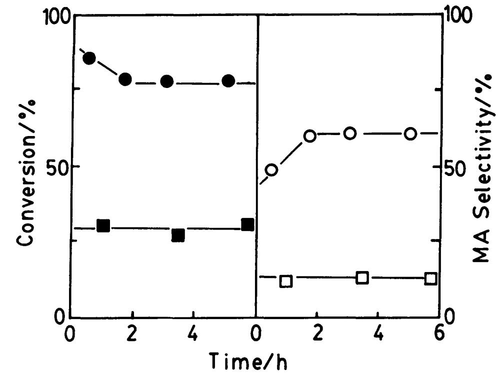

Fig. 5. Activity and selectivity for oxidation of butane at 440 °C.
●○; $(VO)_2P_2O_7$, ■□; β-$VOPO_4$.
Reaction conditions; butane 1.5%, O_2 17%, $W/F=0.67\times10^3$ g·h·mol^{-1}.

in Fig. 2. Figure 3 shows the infrared spectra of the catalysts in the region of 800—1200 cm^{-1}. This region corresponds to the stretching modes of P–O and V=O. The spectra for α-, β-$VOPO_4$ and $(VO)_2P_2O_7$ were in agreement with those reported in the literature.[15,21] The spectra of X_1 and X_2 (1170, 1080, and 955 cm^{-1}) were similar to each other.

XPS spectra of β-$VOPO_4$ and $(VO)_2P_2O_7$ are shown in Fig. 4. The peaks at 526.1 and 519 ev for β-$VOPO_4$ are assigned to $2p_{1/2}$ and $2p_{3/2}$ of vanadium (V) and those at 524.6 and 517.7 eV to $2p_{1/2}$ and $2p_{2/3}$ of vanadium (IV).[22] Although the surfaces of metal oxides are sometimes in more oxidized states than in the bulk, *e.g.*, Fe_2O_3 at the surface of Fe_3O_4,[23] the oxidation states of the catalysts prepared in the present study were very close to those in the bulk. Therefore, it is probable that the crystalline bulk structures were maintained on the surface of these catalysts. The XPS spectra of β-$VOPO_4$ and $(VO)_2P_2O_7$ did not change after they were used for the oxidation of butane.

3. Catalytic Oxidation of Butane to Maleic Anhydride (MA). Catalysts 1 to 10 (catalyst numbers in Tables 2—4) were used for the oxidation of butane. Typical time courses of the reaction over β-$VOPO_4$ (catalyst 3) and $(VO)_2P_2O_7$ (catalyst 10) are shown in Fig. 5. β-$VOPO_4$ showed a constant conversion and selectivity from the beginning of the reaction. α-$VOPO_4$ (catalyst

Table 5. Changes of phases and valence during reaction

Phase	W/F[a]	Conv.	Rate[b]	Selectivity/C_4-base%			Phase after reaction[c]	Valence of V[d]	Cat. No.
		%		CO	CO_2	MA			
α-$VOPO_4$	0.67	53	7.8	57	25	18	α-$VOPO_4$	4.99	1
β-$VOPO_4$	0.67	62	9.1	61	21	18	β-$VOPO_4$	—	2
β-$VOPO_4$	0.67	31	4.6	61	25	14	β-$VOPO_4$	4.99	3
β-$VOPO_4$	0.67	14	2.1	53	27	20	β-$VOPO_4$	—	4
X_1	0.67	59	8.7	44	16	40	$\alpha+X_2$	4.97	5
X_2	0.67	52	7.7	41	15	44	$\alpha+X_2$	4.99	6
Amorphous	0.67	61	9.0	69	15	16	$\alpha+\beta$	—	7
Amorphous	0.54	15	2.7	51	5	44	$X_2+\alpha$	—	8
$(VO)_2P_2O_7$	0.33	27	7.9	20	8	72	$(VO)_2P_2O_7$	4.05	9
$(VO)_2P_2O_7$[e]	0.13	35	25.8	23	10	67	$(VO)_2P_2O_7$	4.11	10

a) 10^3g·h·mol^{-1}. b) 10^{-4}mol(g·h)$^{-1}$. c) In the case of mixtures, the main phases are given in the first place. d) After reaction. e) After washing with water (see text).

1) showed a result similar to β-$VOPO_4$. In the case of $(VO)_2P_2O_7$, the activity and selectivity changed slightly at first, and became constant after 2 h. For X_1 and X_2, both the activity and selectivity gradually increased for an initial 3 h. Changes were also observed for amorphous catalysts.

The catalytic activity and selectivity for the oxidation of butane at 440 °C are summarized in Table 5. Data for the stationary state are given in this table. The $(VO)_2P_2O_7$ which was washed and recalcined was most active; however, the catalytic activity was more or less similar when normalized to surface area. The activity of β-$VOPO_4$ was almost proportional to the surface area of the catalysts. In contrast, the selectivity to MA greatly depended on the structure of the catalyst. It was especially high for $(VO)_2P_2O_7$ (about 70%). X_1 and X_2 showed moderate selectivity (40%), and the selectivity was low for α- and β-$VOPO_4$ (20%).

Phase and valence changes of vanadium during the reaction were determined as summarized in Table 5. The XRD patterns changed little after the reaction in the cases of α-, β-$VOPO_4$ and $(VO)_2P_2O_7$. However, X_1 and X_2 changed into mixtures of α-$VOPO_4$ and X_2, for which the compositions were similar. Amorphous phases, catalysts 7 and 8, also changed to mixed phases. The oxidation states of vanadium remained unchanged for α-, β-$VOPO_4$, X_1, X_2 and $(VO)_2P_2O_7$, but those for amorphous phases increased to about five.

Figure 6 shows the effects of W/F on the conversion and the selectivity to MA obtained for $(VO)_2P_2O_7$ and β-$VOPO_4$, where W is the weight of catalyst and F is the flow rate of butane. The selectivity was nearly constant in this range of conversion, although a slight decrease was observed at a low conversion level for $(VO)_2P_2O_7$.

The effects of the reaction temperature on the reaction rate and selectivity are shown in Fig. 7 for $(VO)_2P_2O_7$. The conversion was adjusted to about 40% in order to compare the selectivity, except for the reaction at 250 °C. The rate at 250 °C was so low that a higher conversion was not attained. The selectivity increased as the reaction temperature decreased and was about 90% at 250 °C.

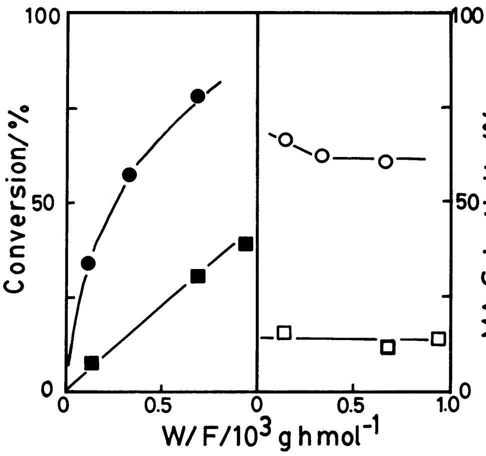

Fig. 6. Effect of W/F on conversion and selectivity to maleic anhydride for oxidation of butane.
●○; $(VO)_2P_2O_7$, ■□; β-$VOPO_4$.
Reaction conditions; 440 °C, butane 1.5%, O_2 17%.

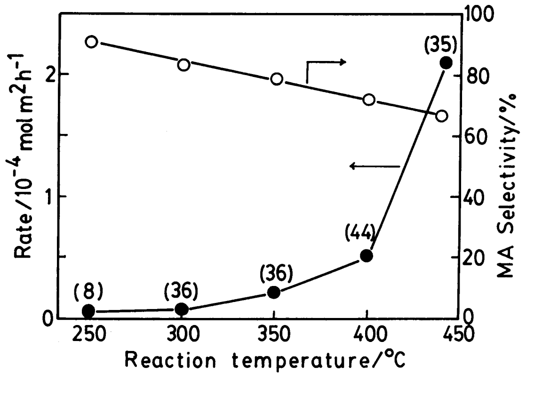

Fig. 7. Effect of reaction temperature on rate and selectivity for oxidation of butane over $(VO)_2P_2O_7$.
Reaction conditions; butane 1.5%, O_2 17%.
Figures in parentheses are % conversions.

The effect of the valence of vanadium on the catalytic properties was examined using catalysts which were prereduced by H_2. Prior to the reaction, β-$VOPO_4$ (catalyst 3) and X_1 were reduced with H_2 in a closed circulation system (200 cm^3) at 400 °C until the average

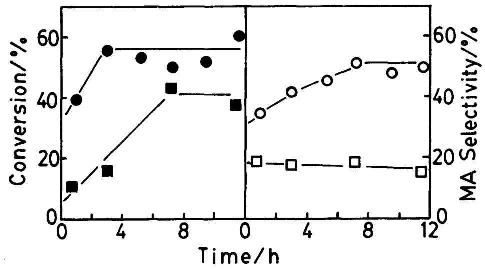

Fig. 8. Variation of activity and selectivity for oxidation of butane over reduced catalysts at 440 °C with reaction time.
Reaction conditions; butane 1.5%, O_2 17%, $W/F = 0.67\times10^3\,\mathrm{g\cdot h\cdot mol^{-1}}$.
● ○; reduced X_1, ■ □; reduced β-$VOPO_4$.

valence of vanadium became four. After the treatment, the structure of β-$VOPO_4$ and X_1 changed to amorphous. As shown in Fig. 8, the activity increased with the reaction time for both catalysts and became constant at later stage. The rates as well as the selectivity at the steady state were comparable with those of corresponding unreduced catalysts. After the reaction, the reduced β-$VOPO_4$ showed very weak peaks corresponding to β-$VOPO_4$ and the reduced X_1 showed XRD peaks corresponding to α-$VOPO_4$ and $(VO)_2P_2O_7$.

Discussion

1. Structure of V–P Oxides with P/V=1. Several structures have been reported for crystalline phases of V–P mixed oxide catalysts with a P/V ratio close to unity. These phases have recently been reviewed by Delmon and Hodnett.[24] Among them, only α-$VOPO_4$, β-$VOPO_4$, and $(VO)_2P_2O_7$ are structures which were determined by XRD analyses of single crystals.

The phases which have been claimed to be efficient catalysts for the selective oxidation of butane to MA are, for example, phase X of ICI[12] and B phase of Chevron.[11] The XRD powder patterns of X and B closely resemble those of α-$VOPO_4$ and $(VO)_2P_2O_7$, respectively. The phases X_1 and X_2 showed XRD patterns very similar to β* phase reported by Delmon and Hodnett[8,24,25] and to B′ phase of ICI,[26] respectively. Therefore, so far there have been reported five phases of V–P mixed oxide catalysts (P/V=1), *i. e.*, α-$VOPO_4$, β-$VOPO_4$, $(VO)_2P_2O_7$ (=B phase), X_1 (=β* phase), and X_2 (=B′ phase). However, it must be kept in mind that catalysts showing similar XRD patterns are often different in crystallinity and purity and sometimes exhibit quite different activity and selectivity.

2. Preparation of Single Crystalline Phases. The preparation processes of the V–P oxides studied in the present work (Tables 2 and 3) are summarized in Fig. 9. As discussed below, these results demonstrate that the factors investigated, *i,e.*, the kind of precursors, the heating rate, the temperature of calcination, and the atmosphere of calcination, are all important factors in determining the resultant structure of catalysts.

2.1 Calcination in the Oxidizing Atmosphere: First of all, it is noteworthy that α- and β-$VOPO_4$ were respectively formed as single phases (judged from XRD powder patterns), by controlling the heating rate. Trifiro *et al.* reported that α-$VOPO_4$ was transformed to β-$VOPO_4$ when α-$VOPO_4$ was heated for a prolonged period at a high temperature,[21] so that β is likely the more stable phase at high temperatures. Bordes and Courtine[15] reported only the formation of β-$VOPO_4$ by the calcination of P-I in O_2. However, the present study has revealed that α-$VOPO_4$ was exclusively formed when the temperature was raised slowly. It is probable that α-$VOPO_4$ is the phase which crystallizes readily at lower temperatures and that once α-phase is formed it is not easily transformed to the β-phase.

P-I tended to melt at 400—450 °C when it was calcined in O_2; sometimes, the gas flow decreased sharply. In these cases, mixtures of α- and β-phases were often obtained. To avoid this phenomenon, we utilized a wide glass tube and raised the temperature gradually while monitoring the rate of gas flow.

Thus, it is important for the preparation of single crystalline phases to control the rate of temperature rise of the calcination process. Trifiro *et al.*[21] also indicated that the heating rate had a significant influence

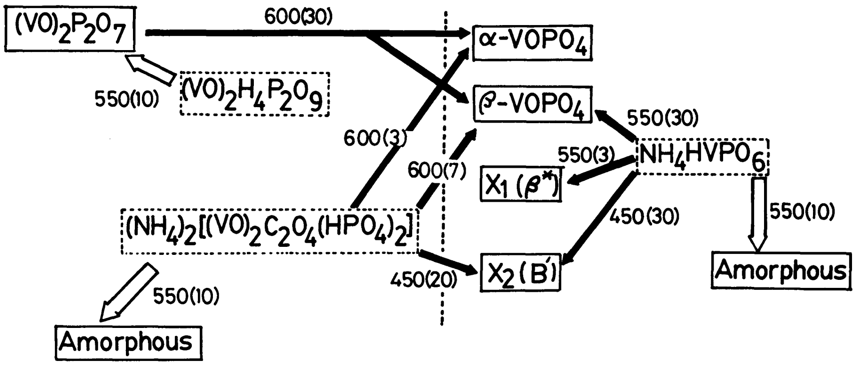

Fig. 9. Preparation processes of V–P oxides.
➡; Calcination in O_2, ⇨; Calcination in N_2.
Figures attached to arrows are calcination temperature and are heating rate (°C $\mathrm{min^{-1}}$, in parentheses).

on the resultant phase.

From P-II (in which vanadium was pentavalent), β-VOPO$_4$, X$_1$, and X$_2$ were respectively obtained by controlling the calcination temperature and the heating rate (Table 2). These results are different from those of Bordes and Courtine[15] who reported the formation of α-VOPO$_4$. Probably, the detailed conditions of the preparation were different, although they are not described in their paper. X$_1$ and X$_2$ crystallized at lower temperatures and were transformed into β-VOPO$_4$ when calcined at high temperatures. As described above, the X$_1$ phase showed a XRD pattern similar to the β^* phase which Delmon and Hodnett obtained as mixtures with other phases. They speculated that vanadium in this phase was quadruvalent on the basis of the fact that the fraction of the β^* phase and the average valence state of vanadium changed somewhat in parallel with the calcination time. However, the X$_1$ phase (=β^*), which was obtained almost as a single-crystalline phase, has vanadium(V) as determined by redox titration. Although the structures of X$_1$ and X$_2$ are not known, it appears probable that they are heteropoly acids with a similar structure (if their solubility in water and the acidic nature of their solutions are considered).

P-III formed mainly (VO)$_2$P$_2$O$_7$ by calcination in air; vanadium (IV) was only partially oxidized to vanadium (V) in contrast to P-I. As described below, due to a similarity in structure, P-III is easily transformed to (VO)$_2$P$_2$O$_7$. This easy transformation may be the reason why the oxidation of vanadium(IV) took place to a much smaller extent than P-I. By calcination at high temperatures, oxidation proceeded progressively to form β-VOPO$_4$ or X$_1$. Therefore, it is necessary for a preparation of pure (VO)$_2$P$_2$O$_7$ to calcine P-III in the absence of O$_2$.

2.2 Calcination in the N$_2$ Flow: The average oxidation states of vanadium in the amorphous phases which were obtained by calcination in N$_2$ of P-I and P-III were less than four, presumably due to the reduction of catalyst by the NH$_3$ present in the precursors. Bordes and Courtine[15] reported the formation of (VO)$_2$P$_2$O$_7$ from P-I. As described above, the phase formed by the calcination of P-I sensitively varies depending on the calcination conditions.

P-III was transformed into (VO)$_2$P$_2$O$_7$ while keeping the valence of vanadium. This is because there was neither a reducing reagent like NH$_3$ nor an oxidizing reagent. As far as XRD is concerned, (VO)$_2$P$_2$O$_7$, thus formed, was pure. According to the structure of P-III determined recently by Torardi and Cababrese,[20] P-III ((VO)$_2$H$_4$P$_2$O$_9$) and (VO)$_2$P$_2$O$_7$ have a very similar structure (Fig. 10). This may be the reason why apparently pure (VO)$_2$P$_2$O$_7$ was rather easily obtained from P-III.

It was claimed in a patent[13] that a higher yield of MA was obtained by the recalcination of the catalyst (probably (VO)$_2$P$_2$O$_7$) in air at a high temperature followed by washing with water and calcination at a lower temperature. The present study (Fig. 1) indicates that amorphous or a less-crystalline phase, contained as an impurity, turned to the X$_1$ phase by calcination in O$_2$ and that the X$_1$ phase, thus formed, was washed out, resulting in a highly crystalline and pure (VO)$_2$P$_2$O$_7$.

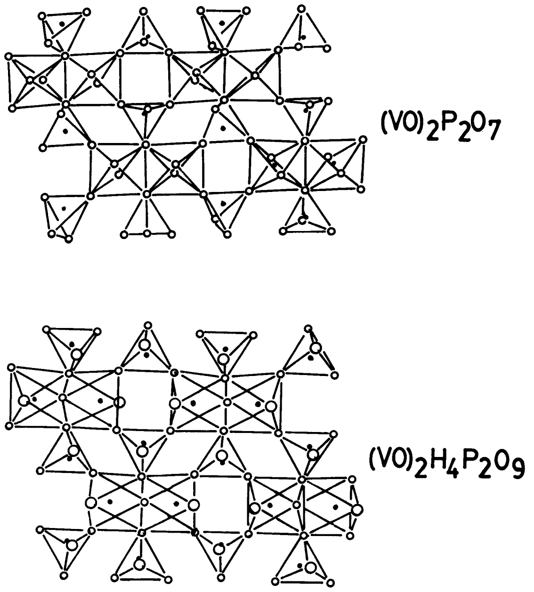

Fig. 10. Structure of (VO)$_2$P$_2$O$_7$ and (VO)$_2$H$_4$P$_2$O$_9$.[20]

2.3 Purity and Crystallinity: Each α- and β-VOPO$_4$, as well as (VO)$_2$P$_2$O$_7$, prepared in this work by carefully controlling the preparation conditions showed sharp XRD peaks of their corresponding structures. IR spectra also agreed with those reported in the literature. Therefore, the purity and crystallinity of all of these catalysts are considered to be of the highest level among the catalysts used in the preceding studies.

The fact that the oxidation states of vanadium were close to four for (VO)$_2$P$_2$O$_7$ and five for α- and β-VOPO$_4$ supports this consideration. X$_1$ and X$_2$ are likely to have a similar level of purity, as revealed by XRD patterns and IR spectra together with the oxidation state. Furthermore, an XPS analysis showed that the oxidation state of vanadium on the surface was not different from that in the bulk in the cases of β-VOPO$_4$ and (VO)$_2$P$_2$O$_7$.

3. Efficient Phase for Catalytic Oxidation of Butane to Maleic Anhydride (MA). The catalytic activity and selectivity to MA of each single phase will be phenomenogically discussed. Chevron found a fair correlation between the MA yield and the content of the B phase (=(VO)$_2$P$_2$O$_7$).[11] It was claimed that this phase was the efficient phase, although the highest content of the B phase was obtained at P/V=1.2 and the average valence of vanadium was 4.1—4.5.

Later, ICI indicated that phase X ($\fallingdotseq$ α-VOPO$_4$) was effective[12] and Delmon's group suggested that the β^* phase was also effective,[8] while their catalysts were mixtures. Matsuura suggested that both α-$VOPO_4$ and $(VO)_2P_2O_7$ were good catalysts, since the reaction proceeded by the redox cycle between these two phases.⁶⁾ Recently, a patent from Mitsubishi Chemical Industry indicated that their catalysts with P/V=1 exhibited a high MA yield and had a $(VO)_2P_2O_7$ structure.¹⁴ᶜ⁾

In our present study, as discussed above, catalysts contained single crystalline phases. The P/V ratios were all unity and the vanadium valences were close to four or five. Moreover, $(VO)_2P_2O_7$ was stable and changed little under the reaction conditions. Structural changes of α- and β-$VOPO_4$ were also negligible. Therefore, it is meaningful to compare the catalytic activity and selectivity of the catalysts as given in Table 5. Table 5 shows that the performance as a catalyst was in the order of $(VO)_2P_2O_7 > X_2$, $X_1 > \alpha$-, β-$VOPO_4$; the selectivity to MA was much better for $(VO)_2P_2O_7$ (catalysts 9 and 10), while the rate normalized to the surface area was more or less similar. The positions of X_1 and X_2 are not certain, since no single phase of X_1 or X_2 was observed after use for a reaction.

A possible reason for the different performances between $(VO)_2P_2O_7$ and α-, β-$VOPO_4$ is the oxidation state of vanadium. However, the prereduced catalysts showed only low selectivities (Fig. 8). Also, the selectivity increased with the reaction time when $(VO)_2P_2O_7$ was formed after reaction and it maintained a low level when β-$VOPO_4$ was formed (Fig. 8). Furthermore, amorphous catalysts having low oxidation states of vanadium also showed low selectivities (Table 5). Thus, catalysts containing vanadium(IV) are not always good catalysts. A certain well-defined structure which is stable under the reaction conditions appears to be necessary. Probably, the $(VO)_2P_2O_7$ catalyst was an efficient catalyst since it consisted of a single crystalline phase in which vanadium(IV) was stable under the reaction conditions. The very high selectivity obtained for $(VO)_2P_2O_7$ at a low temperature (Fig. 7) may be meaningful since the secondary reactions of MA are not significant in this reaction.

Matsuura suggested that the reaction proceeded by a redox cycle between $(VO)_2P_2O_7$ and α-$VOPO_4$.⁶⁾ In the present work for purified $(VO)_2P_2O_7$, such a redox cycle was not indicated. Nevertheless, the superiority of $(VO)_2P_2O_7$ is common in the two studies. While Trifiro *et al.*⁹˒¹⁰⁾ also reported that the B-phase ($\fallingdotseq (VO)_2P_2O_7$) showed a good performance, our results were considerably better at high conversion levels. The purity of $(VO)_2P_2O_7$ is a possible reason of this difference. Delmon and Hodnett⁸⁾ recently indicated that the β^* phase ($=X_1$) was the efficient phase. The data obtained for the β^* phase were comparable with the X_1 phase in the present study. The X_1 phase was transformed to X_2 and α-$VOPO_4$ during the reaction (Table 5). If one considers the low selectivity of the α-phase, the pure X_2 phase itself could be a fairly good catalyst.

The variations of activity and selectivity of amorphous catalysts 7 and 8 with reaction time are consistent with the concurrent structural changes. When the amorphous catalyst 7 was used as a catalyst, the conversion increased from about 20% (at 3 h) to 60% (after 12 h), and the selectivity to MA decreased from about 30 to about 20%. The steady activity and selectivity were close to those of α-$VOPO_4$. While the conversion was less than 20% (during 15 h) over the catalyst 8, the selectivity to MA gradually increased with time from 25 to 40% (15 h). This is consistent with the result for X_2.

The authors would like to thank Prof. S. Naito and Dr. C. Egawa (The University of Tokyo) regarding the XPS measurement and Mr. M. Kojima, Mr. T. Kurokawa, and Mr. K. Shibata for experimental work at the preliminary stage of this work. A helpful discussion at this stage with Prof. I. Matsuura (presently Toyama University) is also gratefully acknowledged.

References

1) R. L. Varma and D. N. Saraf, *Ind. Eng. Chem., Prod. Res. Dev.*, **18**, 7 (1979).

2) M. Nakamura, K. Kawai, and Y. Fujiwara, *J. Catal.*, **34**, 345 (1974).

3) M. Ai, T. Niikuni, and S. Suzuki, *Kogyo Kagaku Zasshi*, **73**, 165 (1970).

4) L. Morselli, A. Riva, F. Trifiro, M. Zucchi, and G. Emig, *Chim. Ind.*, **60**, 791 (1978).

5) I. Matsuura, *Hyomen*, **20**, 605 (1982).

6) I. Matsuura, Preprints of the 6th Japan-Soviet Catalysis Seminar, 1981 p. 149.

7) I. Matsuura, *Proc. 8th Intern. Congr. Catal. (Berlin)*, **4**, 473 (1984).

8) B. K. Hodnett, P. Permanne, and B. Delmon, *Appl. Catal.*, **6**, 231 (1983).

9) F. Cavani, G. Centi, and F. Trifiro, *Appl. Catal.*, **9**, 191 (1984).

10) F. Cavani, G. Centi, I. Manenti, A. Riva, and F. Trifiro, *Proc. 9th Iberoamerican Symp. Catal., Lisbon*, **1984**, 973.

11) R. A. Schneider (to Chevron Research Co.), U. S. Patent 3864280 (1975).

12) ICI, *Belg.*, **1978**, 867189.

13) S. Kamimura and M. Murayama (to Mitsubishi Chemical Industries Co., Ltd.), *Jpn. Kokai*, **1979**, 161594.

14) a) M. Otake (to Mitsubishi Chemical Industries Co., Ltd.), *Jpn. Kokai*, **1981**, 45815; b) M. Otake (to Mitsubishi Chemical Industries Co., Ltd.), *Jpn. Kokai*, **1981**, 54215; c) M. Otake (to Mitsubishi Chemical Industries Co., Ltd.), *Jpn. Kokai*, **1982**, 111218.

15) E. Bordes and P. Courtine, *J. Catal.*, **57**, 236 (1979).

16) B. Jordan and C. Calvo, *Can. J. Chem.*, **51**, 2671 (1973).

17) R. Gopal and C. Calvo, *J. Solid State Chem.*, **5**, 432 (1972).

18) J. E. Ropbyhoba and C. A. Lnhge, *Izv. Akad. Nauk SSSR*, **23**, 584 (1978).

19) S. Pulvin, M. Ronis and P. Courtine, *C. R. Acad. Sci. Paris, Ser. C.*, **293**, 585 (1976).

20) C. C. Torardi and J. C. Calabrese, *Inorg. Chem.*, **23**, 1308 (1984).

21) G. Centi, I. Manenti, A. Riva, and F. Trifiro, *Appl. Catal.*, **9**, 177 (1984).

22) C. Blaauw, F. Leenhouts, F. Van der Woude, and G. A. Sawatzky, *J. Phys. C*, **8**, 459 (1975).

23) G. Ertl and K. Wandelt, *Surf. Sci.*, **50**, 479 (1975).

24) B. K. Hodnett and B. Delmon, *Appl. Catal.*, **9**, 203 (1984).

25) B. K. Hodnett and B. Delmon, *J. Catal.*, **88**, 43 (1984).

26) G. J. Hutchings and R. Higgins, *U. S. Patent* 4209423 (1980).